



SEISMIC PERFORMANCE OF HIGH STRENGTH CONCRETE COLUMNS CONFINED WITH HIGH STRENGTH STEEL

Oguzhan BAYRAK¹ and Shamim A. SHEIKH²

SUMMARY

An examination of the relevant provisions of the ACI 318-02 building code clearly indicates that the use of high strength steel as confining reinforcement would clearly help reduce the congestion that may be triggered by high concrete strengths. In addition, with increasing concrete strength CAN3-A23.3-M94, NZS 3101:1995 expressions also require a higher volumetric ratio of confining reinforcement. There could be cases where a high volumetric ratio of confining reinforcement would mean the use of tie spacings that are not practical. NZS 3101:1995 standards allow the use of high strength steel (up to 800 MPa) as tie reinforcement. The research reported herein focuses on the use of high strength steel as confining reinforcement and is aimed at determining the practical limit that the rectilinear ties can be strained to under moderate to high axial load levels and reversed cyclic lateral displacement excursions.

INTRODUCTION

According to the current North American seismic design philosophy, the ability of concrete framed structures to withstand strong ground motions depends mainly on the formation of plastic hinges and their capacities to absorb and dissipate energy without significant loss of strength. For this reason, most building codes attempt to ensure hinging in the beams rather than the columns in order to guarantee stability. However, recent earthquakes and analytical investigations [1,2,3] show that the formation of plastic hinges in columns of a framed structure, at locations other than the column bases at the foundation level, is still possible as a result of a severe earthquake despite the application of the “strong column-weak beam” concept in the design according to various design code recommendations. Therefore, formation of plastic hinges in columns located in moment resisting frames is unavoidable and should be relied on, in order to ensure the stability as well as vertical load carrying capacity of the columns while structures undergo large lateral displacements.

During the last three decades, the use of high strength concrete, HSC, has become popular adding another dimension to the seismic design of concrete structures. The equations that exist in the current design codes [4, 5, 6] were based on experimental results in which normal strength concrete, NSC, was used. It has therefore become imperative that the basic concept behind the code equations and the empirical constants be investigated for the ability of these equations to result in ductile HSC members. An

¹ Ferguson Structural Engineering Laboratory, The University of Texas at Austin, Austin, TX, U.S.A.

² University of Toronto, Toronto, Ontario, Canada.

examination of the provisions of the aforementioned codes indicates that as the concrete strength increases the amount of transverse steel acting as confining reinforcement should increase. For concrete strengths as high as 100 MPa the use of ordinary reinforcing bars with yield strengths around 400 MPa may result in congestion of reinforcement in the potential plastic hinge regions. Hence, the use high strength steel as confining reinforcement needs to be investigated.

BUILDING CODES

In this section various concrete design codes' requirements are reviewed in order to investigate the implications of the use of high strength steel as confining reinforcement. More specifically, current versions of the American, Canadian and New Zealand Codes' relevant provisions are discussed.

ACI 318-02

The current version [4] of the Code requires that the total cross sectional area of rectilinear ties shall not be less than that given by the following equations:

$$A_{sh} = 0.3 s h_c \left[\frac{f_c'}{f_{yh}} \right] \left[\frac{A_g}{A_{ch}} - 1 \right] \quad (1)$$

but not less than

$$A_{sh} = 0.09 s h_c \left[\frac{f_c'}{f_{yh}} \right] \quad (2)$$

where;

s = the spacing of the hoops

h_c = the maximum unsupported length of rectangular hoop measured between perpendicular legs of the hoop,
(= l_h)

f_c' = compressive strength of concrete as measured from standard cylinders

f_{yh} = yield strength of spiral reinforcement

A_g = gross area of the section

A_{ch} = area of concrete core measured out to out of transverse reinforcement

The ACI 318-02 requirements for the confinement reinforcement in circular columns is expressed in terms of the volumetric ratio of spiral steel to core instead of total cross-sectional area. The Code requires that volumetric ratio of spiral steel, ρ_s , shall not be less than that given by the following equations:

$$\rho_s = 0.45 \left[\frac{f_c'}{f_{yh}} \right] \left[\frac{A_g}{A_c} - 1 \right] \quad (3)$$

but not less than

$$\rho_s = 0.12 \left[\frac{f_c'}{f_{yh}} \right] \quad (4)$$

where;

ρ_s = the volumetric ratio of the spiral steel

CAN3-A23.3-M94

The amount of transverse reinforcement suggested by this standard is similar to that required in the ACI 318-02 Code except that the factor 0.09 in Equation 2 is 0.12 in the Canadian Code. In fact, the Canadian Code requirements are similar to those in the 1983 version of the ACI Code.

NZS 3101:1995

According to the NEW Zealand Specifications Spiral or circular hoop reinforcement for columns and piers shall be placed as follows:

The volumetric ratio, ρ_s , expressed as a percentage shall not be less than that given by the greater of the following two equations:

$$\rho_s = \frac{(1 - \rho_t \cdot m)}{2.4} \cdot \frac{A_g}{A_c} \cdot \frac{f_c'}{f_{yt}} \cdot \frac{N^*}{\phi \cdot f_c' \cdot A_g} - 0.0084 \quad (5)$$

where A_g / A_c shall not be less than 1.2 and $\rho_t \cdot m$ shall not be taken greater than 0.4.

$$\rho_s = \frac{A_{st}}{155 \cdot d''} \cdot \frac{f_y}{f_{yt}} \cdot \frac{1}{d_b} \quad (6)$$

where;

ρ_s = ratio of volume of spiral or circular hoop reinforcement to total volume of concrete core measured out-to-out of spirals or hoops

ρ_t = ratio of non-prestressed longitudinal column reinforcement = A_{st} / A_g

A_{st} = total area of longitudinal reinforcement, mm^2

A_g = gross area of section, mm^2

m = $f_y / (0.85 f_c')$

A_c = area of concrete core section measured to outside of peripheral spiral or hoop, (mm^2)

f_c' = specified compressive strength of concrete, MPa

f_{yt} = lower characteristic yield strength of spiral, hoop, stirrup-tie or supplementary cross-tie reinforcement, MPa

f_y = lower characteristic yield strength of non-prestressed reinforcement, MPa

N^* = design axial load at ultimate limit state, N

ϕ = strength reduction factor, $\phi = 0.85$ for flexure with or without axial tension or compression

d'' = diameter of concrete core of circular column measured to outside of spiral or circular hoop, mm

d_b = nominal diameter of bar, wire or prestressing strand, or in a bundle, the diameter of a bar of equivalent area, mm

According to NZS 3101:1995 f_{yt} shall not be taken larger than 800 MPa in equations 5 and 6.

An examination of the code expressions outlined above clearly indicates that the use of higher strength steel as confining reinforcement would clearly help reduce the congestion that may be triggered by high concrete strengths. In other words, with increasing concrete strength all code expressions would require a higher volumetric ratio of confining reinforcement. There could be cases where a high volumetric ratio of confining reinforcement would mean the use of tie spacings that are not practical. NZS 3101:1995 standards allow the use of high strength steel as tie reinforcement. However, the use of high strength steel

is not permitted by the North American codes. This necessitates experimental investigation of the use of high strength steel as confining reinforcement in high strength concrete columns.

EXPERIMENTAL PROGRAM

The specimens used in the test program consisted of a 250 x 350 x 1473 mm (9.8 x 13.8 x 58 in.) column and 508 x 762 x 813 mm (20 x 30 x 32 in.) stub. The column part represented the part of a column in a typical building frame between the section of maximum moment and the point of contraflexure. The stub represented a discontinuity like a beam column joint or a footing. The core area in rectangular specimens was kept constant at 74.4% of the gross area of the column section in all the specimens. The core size, measured from center to center of perimeter ties, was 210 x 310 mm (8.3 x 12.2 in.). Table 1 gives the details of the specimens tested and the level of the axial load applied to each specimen during testing.

Table 1. Details of Test Specimens

Spec.	f_c' (MPa)	Lateral Steel					Longitudinal Steel			Axial Load	
		Size (#)	Spac (mm)	ρ_s (%)	f_{yh} (MPa)	A_{sh} $A_{sh(ACI)}$	No. & Size (#)	ρ_t (%)	f_{yl} (MPa)	P $f_c' A_g$	P P_o
RS-17HT	74.1	8.0 mm	75	1.83	1360*	1.14*	8-20M	2.74	521	0.34	0.33
RS-18HT	74.1	8.0 mm	75	1.83	1360*	1.14*	8-20M	2.74	521	0.50	0.49
RS-19HT	74.2	11.1 mm	75	3.54	1402*	2.20*	8-20M	2.74	521	0.53	0.52
RS-20HT	74.2	11.1 mm	140	1.90	1402*	1.18*	8-20M	2.74	521	0.34	0.33

* : The maximum average tie strain reached in Specimens RS-17HT, RS-18HT, RS-19-HT and RS-20HT is 0.00425. Therefore maximum attainable strength of 850 MPa is used the calculations.

Each specimen was tested under a constant axial load and reversed cyclic lateral displacement excursions until it was not able to maintain the axial load. Prior to the test each specimen was aligned to ensure the concentric application of the axial load. The lateral load was applied at the stub near the stub-column interface (Figure 1). Hence the column test region near the stub was subjected to constant axial force and maximum cyclic shear and moment. In the first cycle the specimen was subjected to 75% of the elastic or yield displacement (Δ_1), which can be defined as the lateral deflection corresponding to the estimated lateral load carrying capacity (V_{max}) on a straight line joining origin and a point about 65% of V_{max} on the lateral load-displacement curve. Both Δ_1 and V_{max} were calculated using theoretical sectional responses of the unconfined columns and integrating curvatures along the length of the specimen. Subsequent displacement excursions consisted of two cycles each at Δ_1 , $2 \Delta_1$, and so on (Figure 2).

Since behavior of reinforced concrete sections and members is not elastoplastic, several definitions for ductility and deformability are available in literature. In this study the ductility parameters suggested by Sheikh and Houry [7] are used to evaluate the performance of the test specimens. This makes the comparison of the results from the current study to the results obtained in the earlier stages of the ongoing research program more meaningful. Figure 3 illustrates definitions of the ductility parameters for a section based on a moment-curvature relationship. Similar ductility parameters can also be developed from shear (V) vs. tip deflection (Δ_t) which will result in μ_Δ , N_Δ , W comparable to μ_ϕ , N_ϕ , and E in Figure 3.

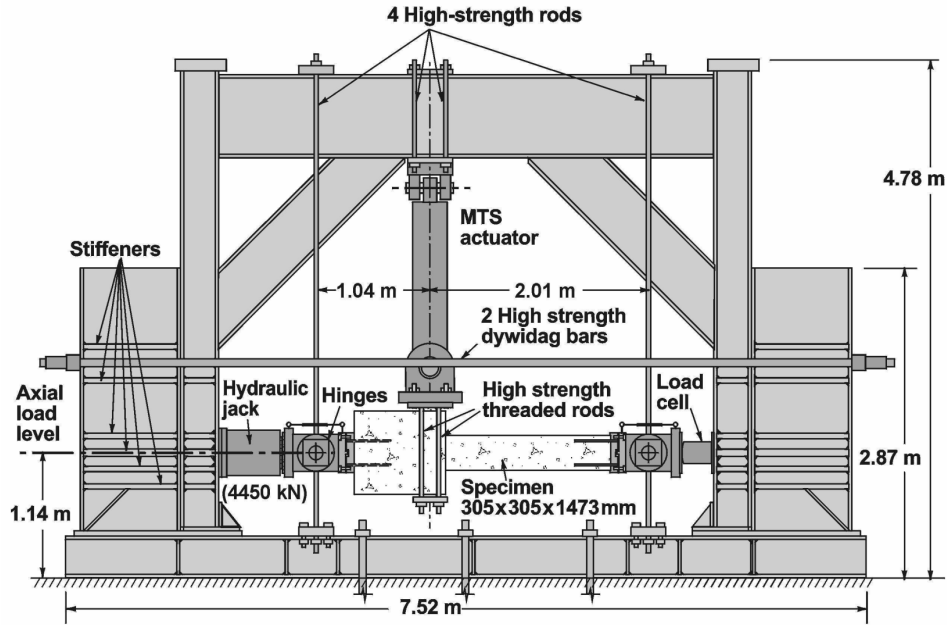


Figure 1. Test Setup

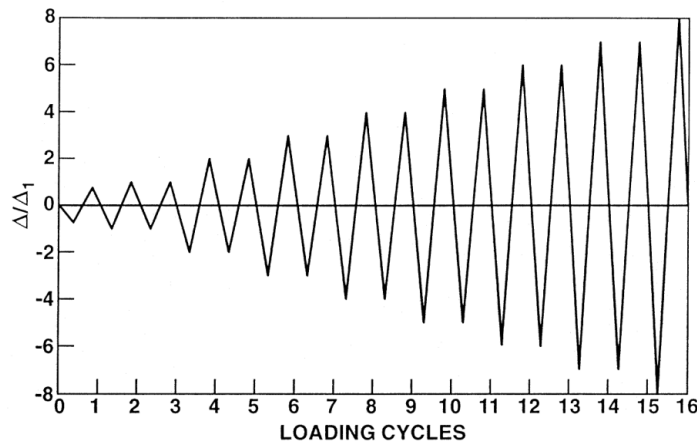


Figure 2. Typical Lateral Displacement History

The definitions for most of the ductility parameters illustrated in Figure 3 are self-explanatory; others however need further explanation. N_{Δ} and N_{ϕ} are cumulative displacement and curvature ductility ratios. These ratios can be used to assess the cumulative amount of inelastic deformations, normalized with respect to yield deformations, experienced by a section or a member. W and E are work damage and energy damage indicators, respectively. By using these two parameters, energy absorption and dissipation characteristics of the test specimens were evaluated. These four parameters can be defined up to the end of a test (in this case subscript “t” is used in Table 2) or up to the cycle in which the strength loss is less than or equal to 20% (in this case subscript “80” is used in Table 2). Ductility parameters of the test specimens are listed in Table 2.

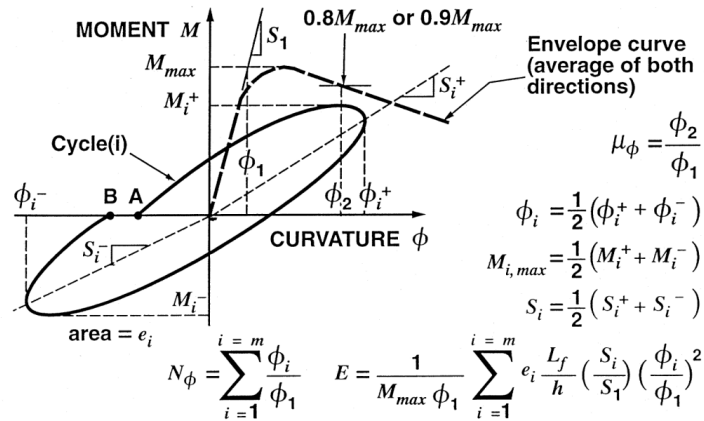
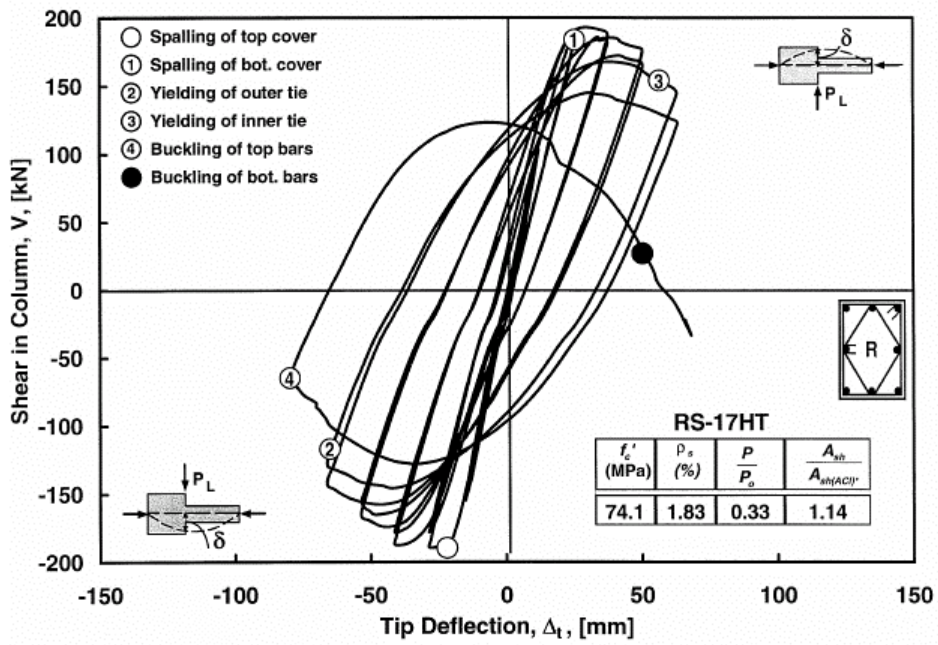


Figure 3. Definitions of Ductility Parameters

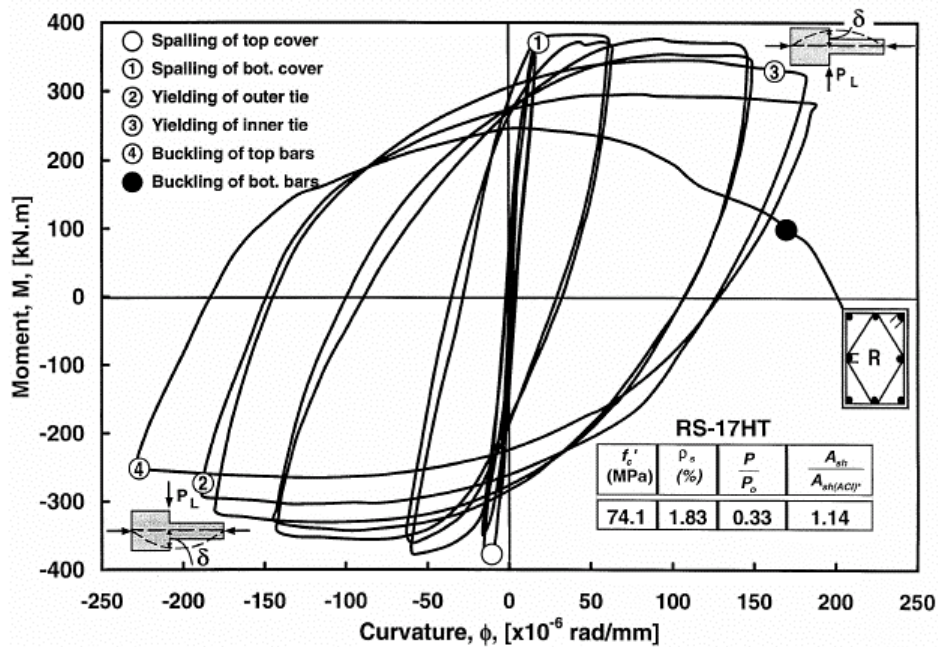
Table 2. Member and Section Ductility Parameters

Specimen	Ductility Factors			Ductility Ratios				Energy Indicators			
	$\mu_{\Delta 80}$	$\mu_{\phi 80}$	$\mu_{\phi 90}$	$N_{\Delta 80}$	$N_{\Delta t}$	$N_{\phi 80}$	$N_{\phi t}$	W_{80}	W_t	E_{80}	E_t
RS-17HT	3.8	16.5	13.9	27	32	51	66	39	51	401	544
RS-18HT	2.8	10.6	9.0	10	12	27	35	23	35	138	229
RS-19HT	6.3	21.7	19.6	18	43	81	174	82	201	1328	2349
RS-20HT	3.8	15.1	11.1	13	22	56	78	32	60	443	1183

Behavior of each specimen can be evaluated in the form of moment vs. curvature and shear force vs. tip deflection relationships. It should be recognized that sectional behavior represented by the $M-\phi$ relationship is of primary concern here because the inelastic deformations concentrate at the plastic hinge once the column is loaded in the post-elastic range. Further lateral displacements will take place mainly as a result of plastic hinge rotation. The moments plotted in Figures 4-7 are those at the failed sections of the columns, including secondary moments caused by the axial load. The curvature was calculated from the deformation readings measured by the upper and lower LVDTs located in the most damaged region within the hinging zone. Spalling of top and bottom cover concrete, yielding of inner and outer ties, and buckling of top and bottom longitudinal bars are marked on the graphs in Figures 4-7. In all specimens, failure did not occur at the column stub connection, although this section was subjected to the maximum moment. Due to the confinement provided by the stub to the adjacent column section, the failure shifted away from the stub.

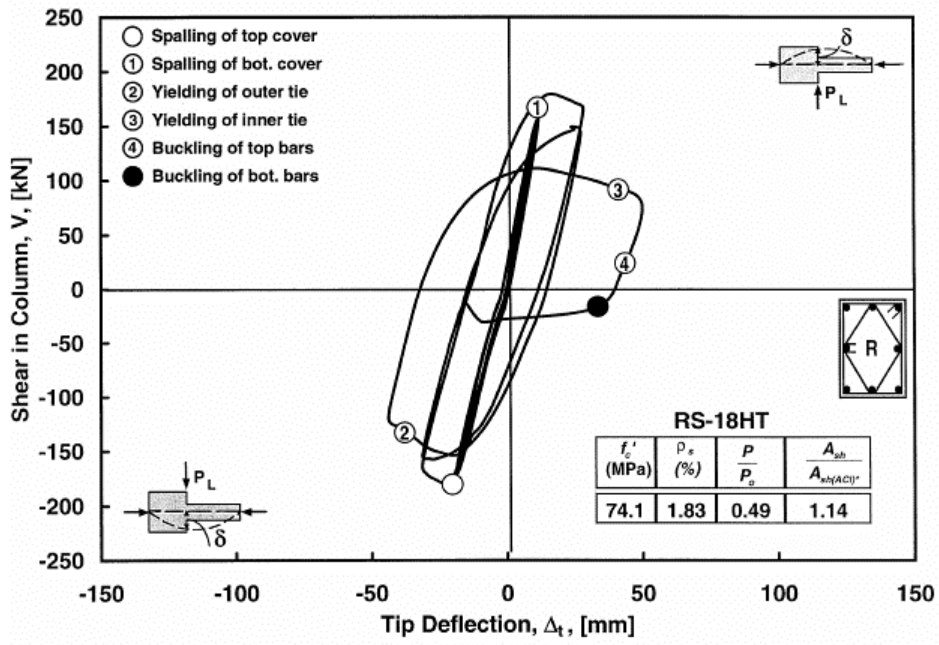


(a) Shear vs. Tip Deflection

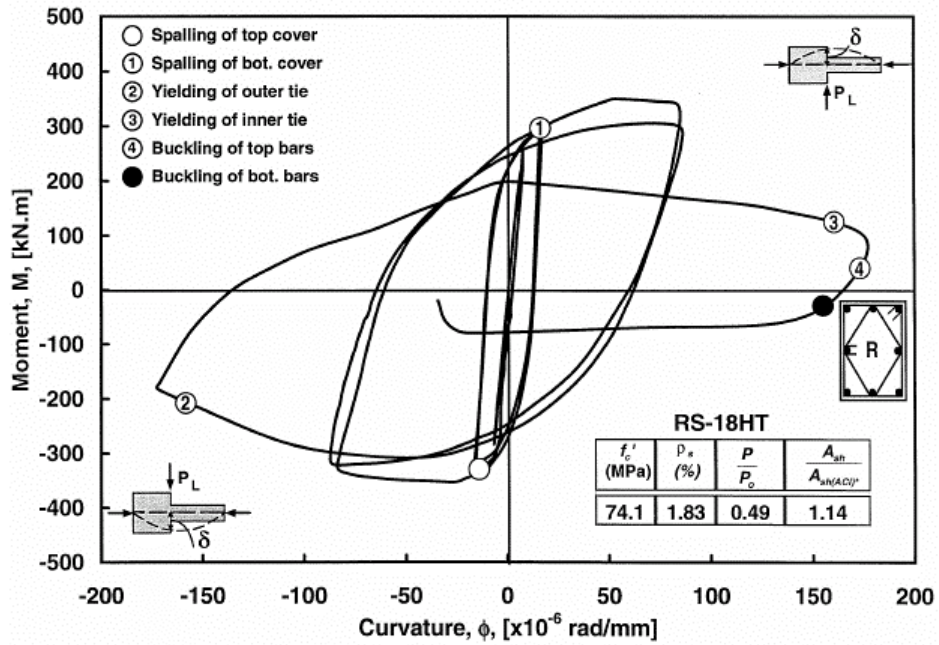


(b) Moment vs. Curvature

Figure 4 Behavior of Specimen RS-17HT

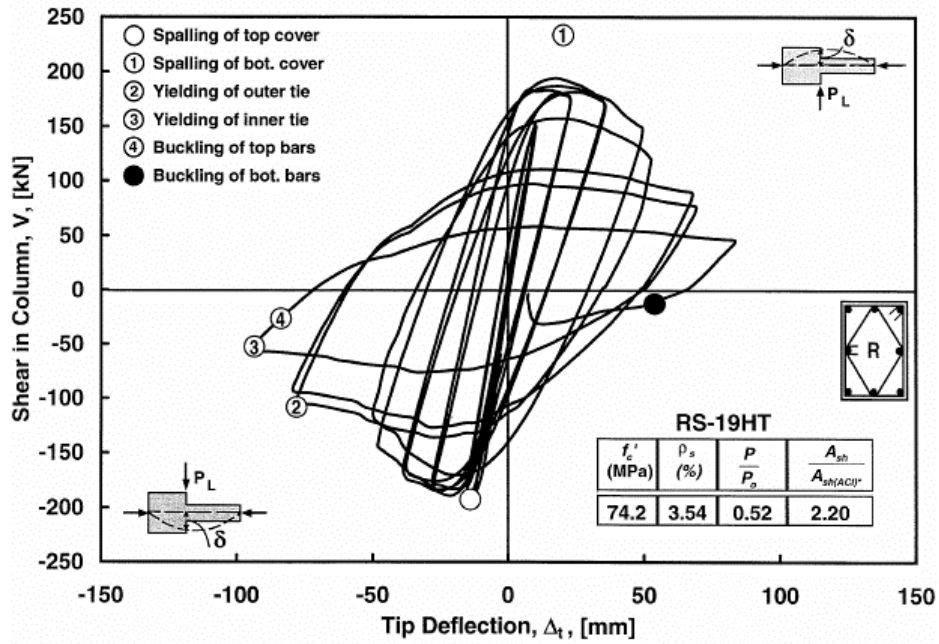


(a) Shear vs. Tip Deflection

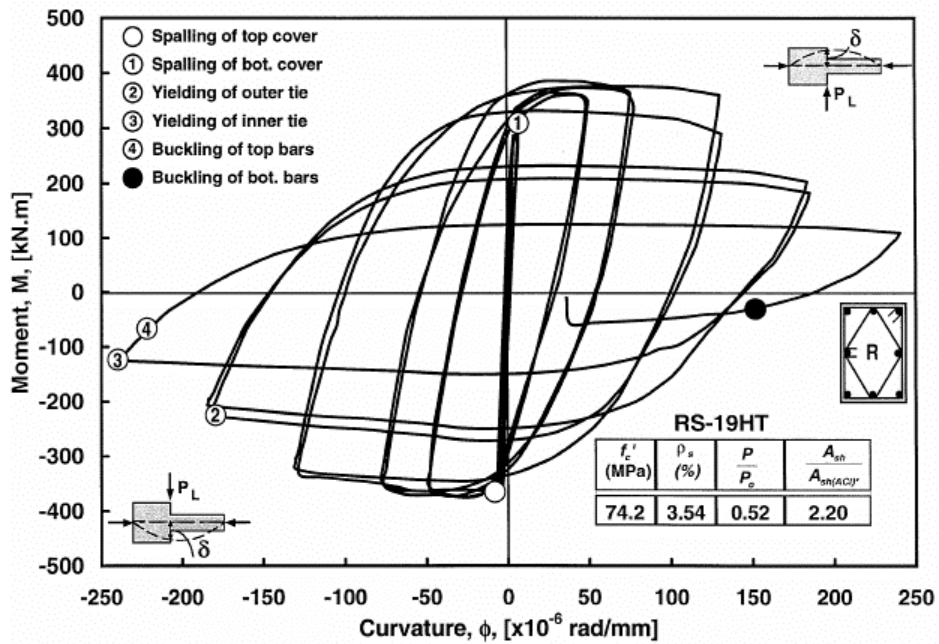


(b) Moment vs. Curvature

Figure 5 Behavior of Specimen RS-18HT

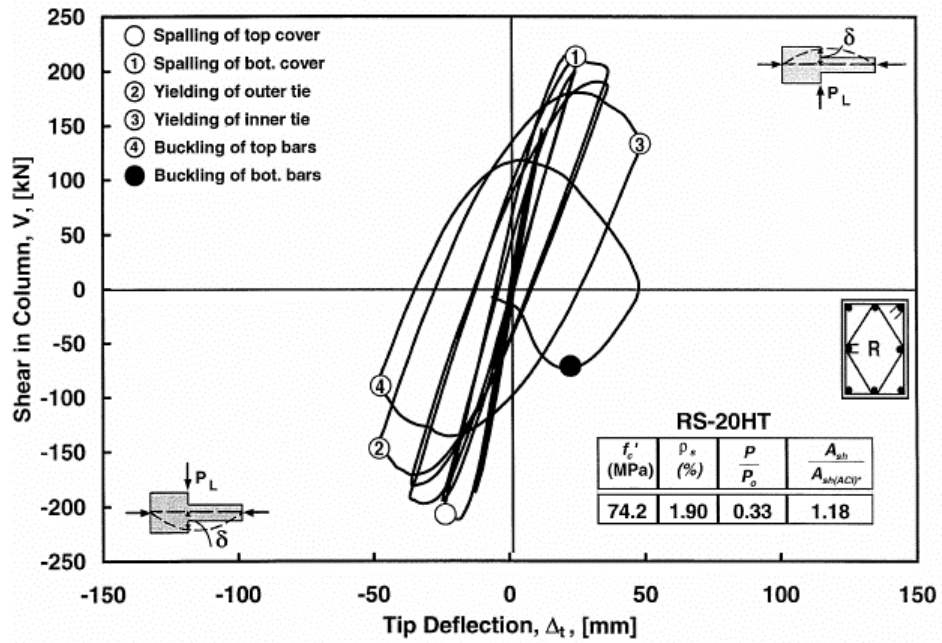


(a) Shear vs. Tip Deflection

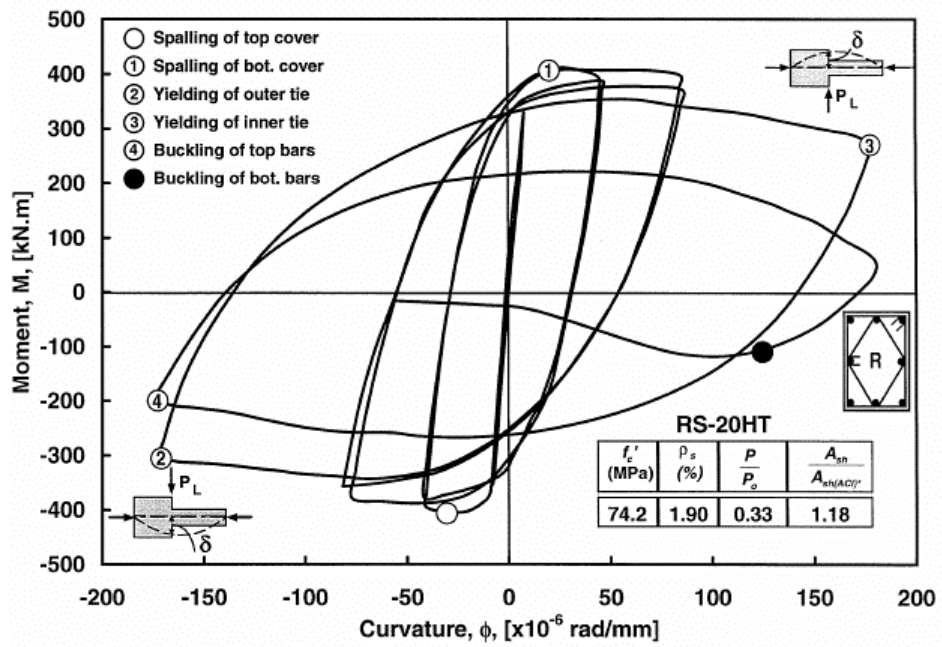


(b) Moment vs. Curvature

Figure 6 Behavior of Specimen RS-19HT



(a) Shear vs. Tip Deflection



(b) Moment vs. Curvature

Figure 7 Behavior of Specimen RS-20HT

TEST OBSERVATIONS

As in NSC specimens [7], first signs of distress in all of the tested specimens were the flexural cracks in the top and bottom concrete cover. The number of cracks formed in the first three cycles seemed to be slightly lower than those in the NSC specimens. The average distance between flexural cracks varied between 55 and 105 millimeters. For all test specimens, top concrete spalled off suddenly just before the first downward peak of the fourth cycle ($\Delta = 2\Delta_1$), and the bottom concrete spalled off at the upward peak of the same cycle. The concrete strains at the time of spalling of cover concrete for all the test specimens were 0.0025, 0.0026, 0.0024 and 0.0027 for Specimens RS-17HT, RS-18HT, RS-19HT and RS-20HT respectively. For columns with closely spaced ties there are two factors that contribute to early loss of cover concrete. First, closely spaced ties formed a weak plane between the concrete core and the cover and resulted in an earlier spalling of concrete cover. Secondly closely spaced ties resulted in high confinement efficiency. The stress-strain behavior of the confined core concrete and the unconfined cover concrete were significantly different and high shear stresses between the core and the cover concrete may have developed in the lateral direction (as the core concrete was restrained against expansion, unlike the cover concrete.)

During the sixth cycle ($\Delta = 3\Delta_1$), cracking propagated to the sides of the columns followed by cover spalling at the sides of the specimen. Flexural cracks formed first in the hinging zone at a distance of approximately 150 mm to 300 mm from the face of the stub and extended in later stages towards the stub. The most extensive damage concentrated at about 200 mm to 300 mm from the face of the stub and extended towards the stub in later stages. Spalling of the cover extended from close to the stub for a distance which ranged between about 350 mm and 600 mm in different specimens. In all the specimens, during the last cycles, buckling of longitudinal bars was observed after yielding of diamond shaped inner ties and perimeter ties, which was an indication of the commencement of failure. For Specimens RS-17HT, RS-18HT, RS-19HT and RS-20HT buckling of longitudinal bars commenced after a maximum average stress of 850 MPa in tie reinforcement was achieved. Hence, in the upcoming sections and in Figure 4-7, the phenomenon referred to as yielding of perimeter and inner ties imply that a tie stress of 850 MPa is achieved in Specimens RS-17HT, RS-18HT, RS-19HT and RS-20HT.

Effect of Amount of Lateral Reinforcement on Column Behavior

An increase in the amount of confining reinforcement made from high strength steel improved the member and section ductility parameters of high strength concrete columns. It can be observed that cumulative curvature ductility ratios and the energy damage indicators are affected more than the curvature ductility factors (Table 2). Specimen RS-18HT had 8.0 mm bar ties spaced at 75 mm resulting in a volumetric ratio of tie reinforcement to core concrete, ρ_s , of 1.83%. Specimen RS-19HT had 11.1 mm bar ties spaced at 75 mm resulting in $\rho_s = 3.54\%$. As a result, the total energy dissipated, E_t , in the plastic hinge region of Specimen RS-19HT was 10.3 times as much as the energy dissipated in the same region of Specimen RS-18HT. The curvature ductility factor, $\mu_{\phi 80}$, of RS-19HT was twice as large as the curvature ductility factor of RS-18HT. The cumulative displacement ductility factor, $N_{\phi 80}$, of RS-19HT was three times larger than that of RS-18HT. The effect of the amount of lateral reinforcement on member ductility parameters is also presented in Table 2. It can be seen from this table that an increase in the amount of high strength transverse reinforcement improved the member ductility parameters of rectangular HSC columns.

Effect of Axial Load on Column Behavior

The effect of axial load on the cyclic behavior of high strength concrete columns confined with high strength steel ties can be evaluated by comparing the responses of Specimens RS-17HT and RS-18HT which are similar in every respect except that P/P_o for Specimen RS-17HT was equal to 0.33 while it was 0.49 in Specimen AS-3HT. Table 2 shows both section and member ductility parameters of these two

specimens. The shear force-tip deflection and moment-curvature behaviors of these specimens are illustrated in Figures 4, and 5 respectively. An increase in axial load from $0.33P_o$ to $0.49P_o$ caused 36% and 35% decreases in the curvature ductility factors, $\mu_{\phi 80}$ and $\mu_{\phi 90}$, respectively. The cumulative curvature ductility ratios showed significant reductions, from 51 to 27 for $N_{\phi 80}$ and 66 to 35 for $N_{\phi 90}$ as a result of increased load. Energy dissipated in Specimen RS-17HT is 2.4 to 2.9 times as much as the energy dissipated in Specimen RS-18HT. As a result of increased axial load in a column, energy-damage indicators appear to be affected the most compared to the other parameters.

Equivalent Plastic Hinge Length

Each test specimen is idealized as a cantilever column. Assuming linear elastic behavior up to the point when yielding occurs at the base of the column, the yield displacement at the tip of the column can be computed as [8]:

$$\Delta_y = \frac{\phi_y L^2}{3} \quad (7)$$

where ϕ_y is the yield curvature at the column base

Assuming that the plastic rotation at the base is concentrated at the center of the plastic hinge, and decomposing the total displacement, Δ_{max} , into two components, Δ_y and Δ_p the following formulation can be introduced.

$$\Delta_{max} = \Delta_y + \Delta_p \quad (8)$$

where Δ_p can be expressed as,

$$\Delta_p = (\phi_{max} - \phi_y)L_p(L - 0.5L_p) \quad (9)$$

Equation 9 [8] assumes that the plastic hinge occurs right at the base of the column. However, because of the additional confinement of the stub, the plastic hinge is shifted away from the stub's face. Therefore, the last term of the Equation 9 should be changed to $(L - 0.5L_p - L_a)$, where L_a is the offset distance by which the plastic hinge is shifted. Equation 9 with the suggested modification and Equation 8 are used to calculate equivalent plastic hinge lengths of the specimens tested; and the results are listed in Table 3. The computations are carried out for all the load cycles in which μ_{Δ} is greater than 4. In any event the length L_p is calculated at least for the last two cycles.

Sheikh and Khoury [7] and Sheikh, Shah and Khoury [8], also reported that the length of the plastic hinge for the specimens tested was approximately equal to the section depth. The plastic hinge length of specimens tested during the course of this study remained approximately equal to the section depth as well. Hence, it is possible to conclude that the use of high strength steel as confining reinforcement did not alter the plastic hinge length of the test specimens. Conversely, the plastic hinge length is not significantly influenced by the strength of confining reinforcement.

Table 3 Equivalent Plastic Hinge Lengths of Specimens

Specimen	Cycle #	Equivalent Plastic Hinge Length		
		L_p (mm)	average	L_p/h
RS-17HT	6	345	296	0.85
	7	321		
	8	276		
	9	276		
	10	284		
	11	276		
RS-18HT	5	334	319	0.91
	6	305		
RS-19HT	6	422	344	0.98
	7	409		
	8	378		
	9	391		
	10	305		
	11	308		
	12	194		
RS-20HT	6	424	349	1.00
	7	399		
	8	341		
	9	233		

Effect of High Strength Confining Reinforcement

Reinforced concrete columns tested in this study concrete was confined by lateral reinforcement in the form of rectangular hoops. Column cross-sections were subjected to axial compression and reversed cyclic bending moments simultaneously. The sections had both longitudinal and transverse reinforcement. At high compressive strains, columns reached a limiting strain when loaded beyond elastic limits, and hence concrete outside the lateral reinforcement spalled off. The core concrete was restrained to expand laterally and the shell concrete was not. Moreover, in high strength concrete columns, due to closely spaced ties, a separation plane between the cover concrete and core concrete formed. This effect was minimized by the use of high strength steel ties; nevertheless its influence on column behavior can not be neglected. In addition, the stress-strain behavior of well-confined concrete was significantly different than that of unconfined concrete. When these two effects were combined, the cover concrete in high strength concrete columns was observed to spall at smaller strains in comparison with normal strength concrete columns. For the columns tested in this study, this strain was smaller than 0.003, the ultimate strain used in ACI 318-02. At this stage due to internal microcracking, core concrete confined in transverse reinforcement tried to expand laterally; in other words there was a tendency for the volumetric strain to increase. Such lateral expansion was restrained by transverse reinforcement through the application of passive lateral pressure on core concrete. At this stage core concrete was no longer uniaxially loaded, but was under triaxial stresses. By monitoring the tie strains continuously, the authors of this paper determined the maximum useful strain experienced by high strength steel ties in a variety of axial load, tie spacing and tie diameter combinations (Table 1).

High strength concrete columns tested in this study were confined with high strength tie steel. The strength of confining reinforcement was as high as 1400 MPa. The use of high strength steel permitted the use realistic tie spacings and reduced the congestion in the plastic hinge region of test specimens. In this way the placement of concrete could be carried out without any difficulties and constructability was improved. In each test specimen a total of 16 strain gauges were installed on the high strength steel ties and tie strains were monitored during the tests. The average of maximum tie strains measured in all the tests was 0.00425. In addition the smallest strain measurement was 0.004. Specimens tested under higher axial loads (Specimens RS18-HT and RS19-HT) experienced slightly higher tie strains than those tested at lower axial load levels (Specimens RS-17HT and RS-20HT.) The experimental data from the tests reported herein supports the use of high strength steel as confining reinforcement. However, there seems to be an upper limit to the strains experienced by the ties in high strength concrete columns. This limit can be conservatively taken as 800 MPa. It is important to appreciate that this finding supports the limit used in the NZS 3101:1995 code.

Mechanical properties of lateral reinforcement have a direct effect on the effectiveness of the confinement. Although the aim is to obtain ductile behavior of the concrete section, this doesn't necessarily mean that the steel used as confinement steel should be ductile with a flat yield plateau. After the transverse steel reaches its yield strain, the expansion of concrete core can continue without any additional restraint until the transverse steel experiences strain hardening, and by that time significant damage would have taken place in the concrete core. Therefore, steel having high yield strength and relatively short yield plateau is preferable to steel having low yield strength and a long yield plateau for use as confinement reinforcement.

CONCLUDING REMARKS

Based on the experimental research summarized in this paper the following conclusions can be drawn:

- The use of high strength confining reinforcement in high strength columns provides an attractive solution to reduce the congestion in the potential plastic hinge regions. An examination of the ACI 318-02, CAN3-A23.3-M94 and NZS 3101:1995 code expressions clearly indicates that the use of higher strength confining reinforcement would clearly help reduce the congestion that may be triggered by high concrete strengths.
- NZS 3101:1995 standards allow the use of high strength steel (up to 800 MPa) as tie reinforcement. The experimental data from the tests reported herein support the use of high strength steel as confining reinforcement and also support the limit of 800 MPa. Conversely rectilinear ties in high strength concrete columns can be strained to strain levels slightly higher than 0.004 and hence 0.004 can be used as a safe lower bound value.
- The plastic hinge length was not influenced by the strength of confining reinforcement. The plastic hinge for the specimens tested was approximately equal to the section depth.
- Mechanical properties of lateral reinforcement have a direct effect on the effectiveness of confinement. Although the aim is to obtain ductile behavior of the concrete section, this doesn't necessarily mean that the steel used as confinement steel should be ductile with a flat yield plateau. After the transverse steel reaches its yield strain, the expansion of concrete core can continue without any additional restraint until the transverse steel experiences strain hardening, and by that time significant damage would have taken place in the concrete core. Therefore, steel having high yield strength and relatively short yield plateau is preferable to steel having low yield strength and a long yield plateau for use as confinement reinforcement.

REFERENCES

1. Park, R., and Paulay, T. (1975), "Reinforced Concrete Structures," John Wiley & Sons, New York, London, Sydney, Toronto.
2. Mitchell, D. and Paultre, P., (1994), "Ductility and Overstrength in Seismic Design of Reinforced Concrete Structures," Canadian Journal of Civil Engineering, V. 21, No. 6, pp. 1049-1060.
3. Bayrak, O., (1995), "High Strength Concrete Columns Subjected to Earthquake Type Loading," M.A.Sc. Thesis, Department of Civil Engineering, University of Toronto, Toronto, Ontario, 239 p.
4. ACI Committee 318, (2002), "Building Code Requirements for Reinforced Concrete and Commentary (ACI 318-02/ACI 318R-02)," American Concrete Institute, Detroit, 429 p.
5. "Code for Design of Concrete Structures for Buildings (CAN3-A23.3-M94)," (1994), Canadian Standards Association, Rexdale, Ontario, 199 p.
6. "Code of Practice for the Design of Concrete Structures," (NZS 3101:1995), (1995), Standards New Zealand, Wellington, Part 1-The Design of Concrete Structures, 256 p.; Part 2 - Commentary on the Design of Concrete Structures, 264 p.
7. Sheikh, S. A., and Houry, S. S., (1993), "Confined Concrete Columns with Stubs," ACI Structural Journal, Vol. 90, No. 4, pp. 414-431.
8. Sheikh, S.A., Shah, D.V., and Houry, S.S., (1994), "Confinement of High-Strength Concrete Columns," ACI Structural Journal, V. 91, No. 1, pp. 100-111.